Auto ADP-ribosylation of NarE, a *Neisseria meningitidis* ADP-ribosyltransferase, regulates its catalytic activities

Monica Picchianti,*,† Mariangela Del Vecchio,* Federica Di Marcello,* Massimiliano Biagini,* Daniele Veggi,* Nathalie Norais,* Rino Rappuoli,* Mariagrazia Pizza,* and Enrico Balducci‡,1

*Novartis Vaccines and Diagnostics, Siena, Italy; †Department of Evolutionary Biology, University of Siena, Siena, Italy; and ‡School of Biosciences and Biotechnologies, University of Camerino, Camerino, Italy

ABSTRACT **NarE is an arginine-specific mono-ADP-ribosyltransferase identified in *Neisseria meningitidis* that requires the presence of iron in a structured cluster for its enzymatic activities. In this study, we show that NarE can perform auto-ADP-ribosylation. This automodification occurred in a time- and NAD-concentration-dependent manner; was inhibited by novobiocin, an ADP-ribosyltransferase inhibitor; and did not occur when NarE was heat inactivated. No reduction in incorporation was evidenced in the presence of high concentrations of ATP, GTP, ADP-ribose, or nicotinamide, which inhibits NAD-glycohydrolase, impeding the formation of free ADP-ribose. Based on the electrophoretic profile of NarE on auto-ADP-ribosylation and on the results of mutagenesis and mass spectrometry analysis, the auto-ADP-ribosylation appeared to be restricted to the addition of a single ADP-ribose. Chemical stability experiments showed that the ADP-ribosyl linkage was sensitive to hydroxylamine, which breaks ADP-ribose-arginine bonds. Site-directed mutagenesis suggested that the auto-ADP-ribosylation site occurred preferentially on the R^7 residue, which is located in the region I of the ADP-ribosyltransferase family. After auto-ADP-ribosylation, NarE showed a reduction in ADP-ribosyltransferase activity, while NAD-glycohydrolase activity was increased. Overall, our findings provide evidence for a novel intramolecular mechanism used by NarE to regulate its enzymatic activities.—Picchianti, M., Del Vecchio, M., Di Marcello, F., Biagini, M., Veggi, D., Norais N., Rappuoli, R., Pizza, M., Balducci, E. Auto ADP-ribosylation of NarE, a *Neisseria meningitidis* ADP-ribosyltransferase, regulates its catalytic activities. *FASEB J.* 27, 4723–4730 (2013). www.fasebj.org**

Key Words: NAD · NAD-glycohydrolase · pathogenesis

Neisseria meningitidis is a gram-negative opportunistic pathogen capable of producing life-threatening infections, such as meningitis and septicemia (1). We have identified an open reading frame in the *N. meningitidis* genome that codes for the ADP-ribosyltransferase NarE, which shares the molecular signature and biochemical features with the ADP-ribosyltransferases (ARTs) from *Vibrio cholerae* and *Escherichia coli* (2). Mono-ADP-ribosylation is a covalent post-translational modification catalyzed by ARTs that plays a role in many physiological and pathological situations (3). ARTs bind β-nicotinamide adenine dinucleotide (NAD) as a substrate and transfer a single ADP-ribose unit to protein/peptide targets coupled to the release of nicotinamide (NAM). In pathogenic bacteria, the attachment of a bulky ADP-ribose by ADP-ribosylating toxins generally modifies the natural function of the target protein, causing various deleterious effects within the host cell (4). The presence of *narE* in hypervirulent strains such as MC58 suggests its involvement in *N. meningitidis* pathogenesis (5). However, no evidence of NarE toxic activity has been provided so far. We have shown that NarE catalyzes arginine (R)-specific ADP-ribosylation and NAD-glycohydrolysis, transferring the ADP-ribose to water (6). A recently discovered feature of NarE is the presence of an iron-sulfur (Fe-S) center that we identified for the first time in a member of the ART family (7). The iron coordination site has been recently resolved, and the amino acids, 2 cysteines (C^{67} and C^{128}) and 2 histidines (H^{46} and H^{57}) that bind iron and zinc have been identified (8). Interestingly, the lack of assembly of the iron-binding site with iron strongly reduced the transferase activity of NarE, while it affected the hydrolase

Abbreviations: ART, ADP-ribosyltransferase; biotin-NAD, 6-biotin-17-NAD; B-PER, bacterial protein extraction reagent; CT, cholera toxin; ECL, enhanced chemiluminescence; IPTG, isopropyl-1-β-D-thiogalactopyranoside; MES, 2-(*N*-morpholino) ethanesulfonic acid; NAD, β-nicotinamide adenine dinucleotide; NADase, NAD-glycohydrolase; NAM, nicotinamide; Ni-NTA, nickel-nitriloacetic acid; TCA, trichloroacetic acid; WT, wild type

[1] Correspondence: Centro Ricerche Novartis Vaccines and Diagnostics, Via Fiorentina 1, 53100 Siena, Italy. E-mail: enrico.balducci@novartis.com

doi: 10.1096/fj.13-229955

This article includes supplemental data. Please visit *http://www.fasebj.org* to obtain this information.

activity only marginally (7). In the present report, we show that NarE can perform auto-ADP-ribosylation on R^7 inserted residues. Auto-ADP-ribosylation of NarE consistently reduced the transferase activity, while enhancing the ability to hydrolyze NAD. Thus our data indicate that auto-ADP-ribosylation could be a means to modulate NarE activities in response to its substrate NAD.

MATERIALS AND METHODS

Materials

[Adenine-U-^{14}C]NAD (274 mCi/mmol), [carbonyl-^{14}C]NAD (53 mCi/mmol), and [adenylate-^{32}P]NAD (1000 Ci/mmol) were purchased from Amersham (Arlington Heights, IL, USA); 6-biotin-17-NAD (biotin-NAD) from Trevigen (Gaithersburg, MD, USA); streptavidin HRP-conjugate from Southern-Biotech (Birmingham, AL, USA); MHAB N45 filter plates from Millipore (Billerica, MA, USA); isopropyl-1-thio-β-D-galactopyranoside (IPTG) from Calbiochem (La Jolla, CA, USA); and Bradford reagent for protein quantification and Dowex AG1-X2 from Bio-Rad (Richmond, CA, USA). Bacterial protein extraction reagent (B-PER) was from Pierce (Rockford, IL, USA), and SimplyBlue Safe Stain was from Invitrogen (Carlsbad, CA, USA). All other reagents used in this study were purchased from Sigma-Aldrich (St. Louis, MO, USA).

Overexpression and purification of recombinant wild-type (WT) and mutant NarE

Recombinant NarE was produced by growing *E. coli* BL21 (DE3) transformed with pET21b$^+$ plasmid carrying the *narE* gene (6) overnight at 37°C. Recombinant NarE was purified as described previously (7). Briefly, expression of *narE* gene was induced by addition of 1 mM IPTG. After 3 h induction at 25°C, cells were harvested by centrifugation and resuspended in B-PER using a ratio of 10 ml for 3 g of pellet in the presence of 0.1 mM $MgCl_2$, 100 U of DNase I, and 1 mg/ml of chicken egg lysozyme. The supernatant obtained after centrifugation of the mixture was loaded onto metal nickel-affinity chromatography column [nickel-nitriloacetic acid (Ni-NTA); Pharmacia, Piscataway, NJ, USA; 1.5 μl matrix/ml culture]. Bound proteins were eluted with buffer A (50 mM sodium phosphate buffer, pH 7.4, and 300 mM NaCl) containing 250 mM imidazole. The purification steps were carried out mainly under anaerobic conditions inside a portable glove box saturated with a mixture of N_2 and H_2. When the purification was carried out in aerobic conditions, the protein was used shortly after purification, to prevent iron-cluster disruption by air.

ADP-ribosylation of NarE

NarE was incubated in 50 mM potassium phosphate (pH 7.4) containing 10 μM [adenylate-^{32}P]NAD (10 μCi/assay) in 50 μl final volume. A control reaction containing all the above reagents except [adenylate-^{32}P]NAD was run in parallel. Reactions were started by the addition of NAD, incubated at 30°C for 1 h, and stopped by adding 50 μl of 50% ice-cold trichloroacetic acid (TCA). The proteins were precipitated overnight on ice and collected, centrifuging the samples at 13,000 *g* at 4°C for 30 min. Pellets were solubilized in reducing sample buffer heated to 70°C for 10 min and separated by SDS-PAGE NuPAGE gel system using 2-(*N*-morpholino) ethanesulfonic acid (MES) as running buffer. Radiolabeled proteins were transferred to nitrocellulose membrane and detected by autoradiography, exposing the membrane to X-ray film (Eastman Kodak, Rochester, NY, USA) for 24–48 h at −80°C.

Detection of biotin-ADP-ribosylated-NarE

NarE was modified following the conditions described above, except that 10 μM of biotin-NAD was used instead of 10 μM [adenylate-^{32}P]NAD in a final volume of 20 μl. Recombinant protein was resolved by SDS-PAGE in 4–12% NuPAGE gel using MES as a running buffer and transferred to nitrocellulose using a dry system apparatus (I-Blot; Invitrogen). The membrane was blocked for 1 h with 5% BSA in PBS containing 0.5% Tween-20 (PBS-T), extensively washed, and then incubated in the same buffer containing streptavidin-HRP conjugate (1:10,000 dilution) and mixed for 1 h on an orbital shaker at room temperature. After several washings with PBS-T, bound streptavidin was detected by the enhanced chemiluminescence (ECL) detection system according to the manufacturer's instructions (Bio-Rad).

Immunoblot analysis

Immunoblotting was carried out with primary polyclonal α-NarE antiserum produced in rabbit against recombinant NarE. After several washings with PBS-T, a secondary rabbit α-mouse HRP-conjugated antibody (Jackson Laboratory, Bar Harbor, ME, USA) was added. Bound antibodies were visualized with ECL. Molecular masses were estimated from protein standards included in each SDS-PAGE.

Chemical stability of the protein-ADP-ribosyl linkages

After ADP-ribosylation as described above, with 10 μM [adenylate-^{32}P]NAD (10 μCi/assay) in 50 μl final volume, NarE was precipitated with 50 μl of 50% ice-cold TCA overnight at 4°C. The nature of the ADP-ribose-protein linkage was determined by incubating the precipitated proteins at 37°C in the presence of H_2O, 1 M NaCl, 0.1 M HCl, 10 mM $HgCl_2$ or 1 M NH_2OH (in 0.1 M Tris, adjusted to pH 7 with NH_4OH; refs. 12, 19, 20). After 4 h, the samples were precipitated with 50% TCA (25% final concentration), solubilized in reducing sample buffer, and analyzed as described above.

Site-directed mutagenesis

A PCR-based method was used to generate His-tagged NarE mutants in *E. coli*. The R7K mutant was generated using mutated oligonucleotides containing an *Nde*I or *Xho*I site in the forward or reverse primers (**Table 1**); the mutated gene was cloned into pET21b$^+$. The R33K, R97K and R124K mutants were generated using the site-directed mutagenesis kit by Invitrogen according to the manufacturer's instructions. The C and E mutants were obtained as described previously (7, 8). All the generated mutants were checked by DNA sequence analysis and were expressed as soluble proteins and purified as described previously (7).

MS analysis of ADP-ribosylated-NarE

Intact mass determination was performed using a MALDI-TOF/TOF mass spectrometer (UltraFlex; Bruker Daltonics GmbH, Bremen, Germany). Ions generated by laser desorption at 337 nm (N_2 laser) were recorded at an acceleration voltage of 20 kV in linear mode. In general, ~200 single spectra were accumulated for improving the signal/noise ratio and analyzed by FlexAnalysis 2.4 (Bruker Daltonics).

TABLE 1. *Mutation primers for NarE*

Mutation	Primers, 5′–3′
R7K	F: *CGCGGATCC*CATATGGGAAATTTCTTATATAAAGGCATTAG
	R: *CCCGCTCGAG*GTTAATTTCTATCAACTCTTTAGCAAT
R33K	F: GGTAATAAAGCTGAAGTTGCAATTAAATATGATGGTAAGTTTAAATAT
	R: TGGACCATGTGTAGCTTTACCATCATATTTAAACTTACCATCATA
R97K	F: AATGGCTATATATATGTTTTAAATAAGGATTTGTTTGGTCAATATTCT
	R: ATGTTCAACCTCATATTCAAAAATAGAATATTGACCAAACAAATC
R124K	F: CCAAATGAGAAGGAAGTAACAATCAGAGCTGAAGATTGTGGCTGTATT
	R: TTTAGCAATAATCACTTCTTCAGGAATACAGCCACAATCTTCAGC

Underlined positions indicate a single-nucleotide mismatch where the mutations are inserted. Restriction sites for *Nde*I and *Xho*I are underlined in italics. F, forward; R, reverse.

Briefly, 1 μl of reaction solution (20–60 pmol) was added to 1 μl of a saturated solution of sinapic acid (3,5-dimethoxy-4-hydroxy-*trans*-cinnamic acid) in 30% (v/v) acetonitrile and 0.1% (v/v) trifluoroacetic acid (TFA). Then 2 μl of the analyte/matrix mixture was spotted on a stainless steel sample target and air-dried at room temperature. Protein mass spectra were calibrated using a mix of external Protein Calibration Standard I and II (Bruker Daltonics).

ADP-ribosyltransferase assay

ADP-ribosyltransferase activity of NarE was tested, monitoring the enzymatic transfer of ADP-ribose to polyarginine by a filter plate-based assay (9). Assays were performed in a total volume of 0.3 ml with 0.6 mg of polyarginine and 0.1 mM [carbonyl-^{14}C]NAD (0.05 μCi). After incubation at 30°C, samples were precipitated with 0.3 ml of 50% (w/v) TCA for 30 min on ice. The experiment was performed in quadruplicates (100 μl) in single wells of a mixed cellulose esters filter plate and placed under vacuum conditions. The unreacted [adenine-U-^{14}C]NAD was washed out with 10 vol of 5% (w/v) TCA, and the incorporated radioactivity was measured in a Packard TopCount counter (Packard Instrument Co., Meriden, CT, USA).

NAD-glycohydrolase (NADase) assay

NADase activity was measured with an assay based on NAM release (10). This assay was carried out in 50 mM potassium phosphate buffer (pH 7.5), 0.1 mM [carbonyl-^{14}C]NAD (0.05 μCi) in a total volume of 0.3 ml. Samples (100 μl) after incubation at 30C were applied to 1-ml column of Dowex AG1-X2, and ^{14}C-nicotinamide was eluted with 5 ml of H_2O for liquid scintillation counting.

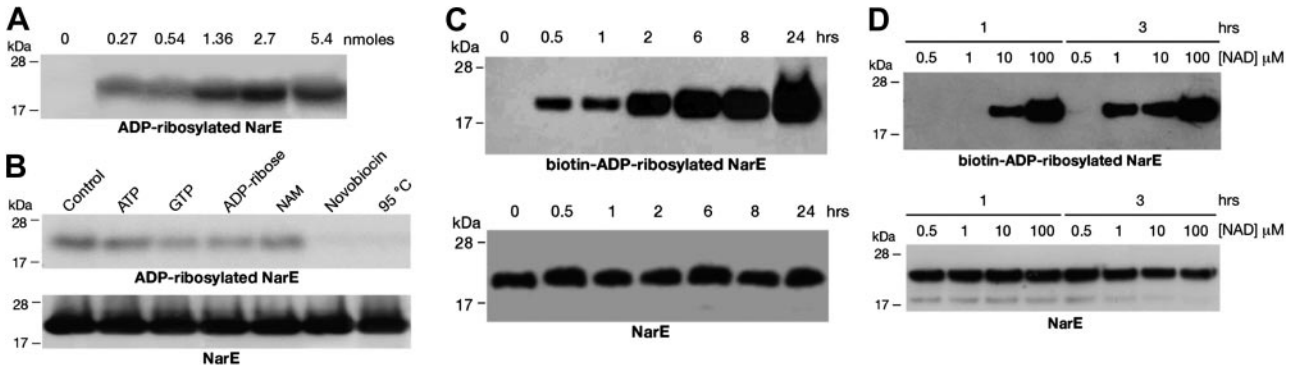

Figure 1. Auto ADP-ribosylation of NarE. *A*) Auto ADP-ribosylation increases with protein concentration. The indicated amounts of NarE were incubated with 10 μM [adenylate-^{32}P]NAD (2 μCi/assay) for 1 h at 30°C. Reactions were run on SDS-PAGE, blotted, and analyzed by autoradiography. *B*) Auto-ADP-ribosylation is inhibited by ADP-ribosylation inhibitors. Purified NarE (5.9 μg, 0.34 nmol) was incubated with 10 μM [adenylate-^{32}P]NAD (2 μCi/assay) for 1 h at 30°C in the absence (control) or presence of 10 mM ATP, GTP, ADP-ribose, or NAM or 5 mM novobiocin. A reaction with heat-inactivated NarE (95°C) was also run. Samples were precipitated in 50% TCA (25% final concentration) for 18 h at 4°C, then centrifuged at 13,000 rpm for 30 min, resuspended in sample buffer, resolved in SDS-PAGE, blotted, and analyzed by autoradiography (top panel). A Western blot of the reaction is also shown (bottom panel). Comparable results were obtained in 3 experiments. *C*) NarE auto-ADP-ribosylation increases as a function of time. Purified NarE (0.5 μg) was incubated at 30°C with 10 μM biotin-NAD in a total volume of 20 μl for the indicated times. After incubation, the ADP-ribosylated NarE was resolved by SDS-PAGE transferred to nitrocellulose. The blot was incubated with streptavidin-HRP conjugate. The biotin-ADP-ribosylated NarE was visualized by chemiluminescence (top panel). After stripping, the blot was incubated with rabbit polyclonal α-NarE, followed by α-rabbit HRP-conjugate, and visualized by chemiluminescence (bottom panel). Positions of molecular mass markers are on the left. Data shown are representative of 2 independent experiments. *D*) NAD concentration enhances the extent of auto-ADP-ribosylation. Affinity-purified NarE (0.5 μg) was incubated at 30°C for 1 and 3 h in 50 mM potassium phosphate buffer (pH 7.5) with the indicated concentrations of biotin-NAD. After incubation, the ADP-ribosylated NarE was resolved by SDS-PAGE in a 10% NuPAGE gel, using MES as running buffer, and transferred to nitrocellulose. After blocking with 5% BSA in PBS-T for 1 h, the blot was incubated with streptavidin-HRP conjugate (1:10,000 dilution) for 1 h at room temperature in the same buffer (upper panel). The control blot was incubated with rabbit polyclonal α-NarE (1:10,000 dilution) and with α-rabbit-HRP conjugate (bottom panel). Visualization was performed by chemiluminescence. Positions of molecular mass markers are on the left. Results are representative of 3 independent experiments with identical results.

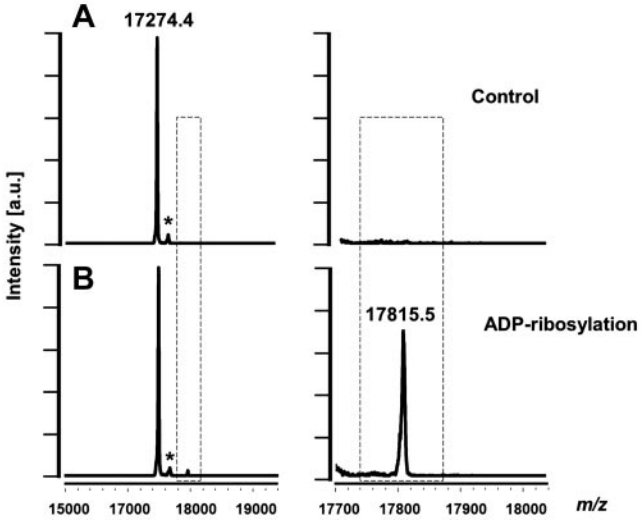

Figure 2. Mass spectrometry analysis indicates that NarE is mono-ADP-ribosylated. Mass spectrometry analysis of NarE (10 μg) after 18 h incubation at 30°C in the absence (*A*) or in the presence of 1 mM NAD (*B*). Asterisk indicates sinapic acid adduct (+206 Da). Right panels show an enlargement of the boxed area in the left panels.

Protein assay

Protein concentration was determined using the Bradford assay kit (Bio-Rad) with BSA (Pierce) as a standard.

RESULTS

Auto-ADP-ribosylation of NarE

To test whether NarE is capable of automodification, we incubated different amounts of purified NarE with 10 μM [adenylate-^{32}P]NAD in the absence of exogenous acceptor. As shown in **Fig. 1*A***, the extent of labeling proceeded in a protein concentration-dependent fashion. To confirm that NarE was auto-ADP-ribosylated and that radioactivity was not incorporated due to a nonenzymatic attachment of NAD, we carried out the automodification reactions in the presence of different inhibitors. As shown in Fig. 1*B*, the labeling of NarE was blocked by the addition of 5 mM novobiocin, an antibiotic known to inhibit transferase reactions (11). Moreover, no radioactivity was incorporated when NarE was heat inactivated. Labeling was slightly decreased by the addition of 10 mM ATP or GTP, which are phosphatase inhibitors (Supplemental Fig. S1). NarE exhibits NADase activity (6), which produces free ADP-ribose that can covalently bind to lysine (K) (12). However, the presence of 10 mM ADP-ribose or 10 mM NAM, a NADase inhibitor (13), slightly affects the incorporation of [adenylate-^{32}P]ADP-ribose in NarE (Supplemental Fig. S1). Overall, these data support the hypothesis that incorporation of ADP-ribose is an enzyme-catalyzed reaction. In the presence of biotin-NAD, the labeling of NarE increased with time (Fig. 1*C*). Automodification also increased as a function of the biotin-NAD concentration (Fig. 1*D*).

Mass spectrometry

To confirm that NarE was ADP-ribosylated, NarE was incubated with or without NAD and analyzed by MALDI-TOF MS, as shown in **Fig. 2**. The unmodified NarE showed an *m/z* value of 17274.4 (Fig. 2*A*), consistent with the expected average mass of the protein lacking the initial methionine (17273.01 Da), while the modified NarE showed an *m/z* value of 17815.5 (Fig. 2*B*). The mass shift of +541 Da between the two forms

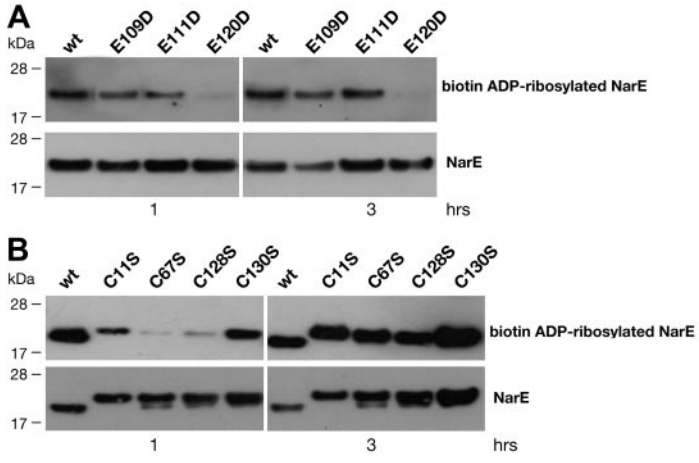

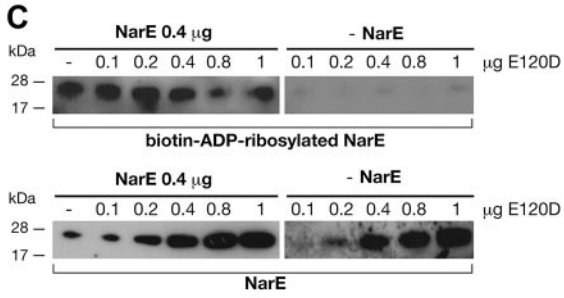

Figure 3. Residues involved in auto-ADP-ribosylation. *A*) E120D is unable to auto-ADP-ribosylate. Mutants with D replacing E at positions 120, 111, and 109 (0.5 μg) were incubated at 30°C for 1 or 3 h in 50 mM potassium phosphate buffer (pH 7.5) with 10 μM biotin-NAD (top panels). Control blots incubated with α-NarE (1:10,000 dilution) are also shown (bottom panels). *B*) C67S and C128S have a reduced ability to auto-ADP-ribosylate. Protein variants C67S and C128S (0.5 μg) were assayed in the same conditions described above (top panels). Control blots incubated with α-NarE are also shown (bottom panels). The different molecular mass of the C mutants may be the result of a partial denaturation. Positions of molecular mass markers are on the left. Data are representative of 3 independent experiments, which gave similar results. *C*) Auto-ADP-ribosylation proceeds by an intramolecular mechanism. NarE (0.4 μg) was incubated with the indicated amount of inactive mutant E120D at 30°C for 1 h in 50 mM potassium phosphate buffer (pH 7.5) with 10 μM biotin-NAD (top left panel). Negative control in the absence of NarE was also performed (top right panel). Control blots with α-NarE polyclonal antibodies (1:10,000 dilution) are also shown (bottom panels).

is in agreement with the covalent addition of a single ADP-ribose moiety. Molecular mass differences corresponding to the addition of a single biotin-ADP-ribose per molecule of NarE were also obtained performing the reaction with biotin-NAD instead of NAD (data not shown). The addition of a single ADP-ribose unit was in agreement with the lack of an appreciable shift observed by SDS-PAGE (Fig. 1*C, D*).

Identification of the residues involved in NarE auto-ADP-ribosylation activity

To get further insights on the molecular basis of automodification, we carried out experiments with different NarE mutants. We have previously identified E^{120} and R^{7} as the crucial residues for NarE catalytic activities (8). Indeed, in the NarE mutant in which E^{120} was replaced with aspartic acid (E120D), no auto-ADP-ribosylation occurred after 1 or 3 h of incubation, while the NarE mutants E111D and E109D, residues that are not involved in catalysis (8), were ADP-ribosylated as WT NarE (**Fig. 3*A***). Previously, we have shown that C^{67} and C^{128}, which are part of an iron-sulfur cluster, are crucial for the transferase but not for the NADase activity of NarE (7). Interestingly, mutants C67S and C128S, which do not have a stable Fe-S cluster, showed a reduced auto-ADP-ribosylation activity after 1 h (Fig. 3*B*) but reached the same level of incorporation compared to the WT or the other CS mutants after 3 h of incubation. Replacement of C^{11} or C^{130} with S resulted in an auto-ADP-ribosylation comparable to WT NarE. Of note, C^{67} and C^{128} residues, which are part of the cluster, still efficiently bind NAD, as evidenced by the presence of NADase activity (7). The E120D mutant, as shown in Fig. 3*A*, is unable to auto-ADP-ribosylate.

Mechanism of the auto-ADP-ribosylation reaction

To clarify whether the ADP-ribosylation of NarE proceeded through an inter- or intramolecular mechanism, we carried out an assay with a fixed amount of NarE and in the presence of increasing amounts of the inactive E120D mutant. As clearly shown in Fig. 3*C*, the incorporation of biotin-ADP-ribose did not correlate with the increase in mutant protein concentration. This result strongly indicates the presence of an intramolecular ADP-ribosylation, ruling out an intermolecular reaction as it happens in the *Clostridium* limosum C3 toxin (14).

Chemical stability of the ADP-ribosyl-NarE linkage

To identify the target amino acid, the auto-ADP-ribosylated ^{32}P-labeled NarE was incubated with NH_2OH, $HgCl_2$, HCl, NaOH or NaCl. A control reaction incubated with H_2O was run in parallel. As shown in **Fig. 4*A***, neutral NH_2OH treatment, which is known to split the ADP-ribosyl–arginine linkages but not the bonds between ADP-ribose and other amino acids (15, 16), and NaOH treatment strongly reduced the intensity of labeling of NarE, suggesting that the ADP-ribosylation occurred at an arginine residue (17). Indeed auto-ADP-ribosylation of cholera toxin (CT), which modifies itself

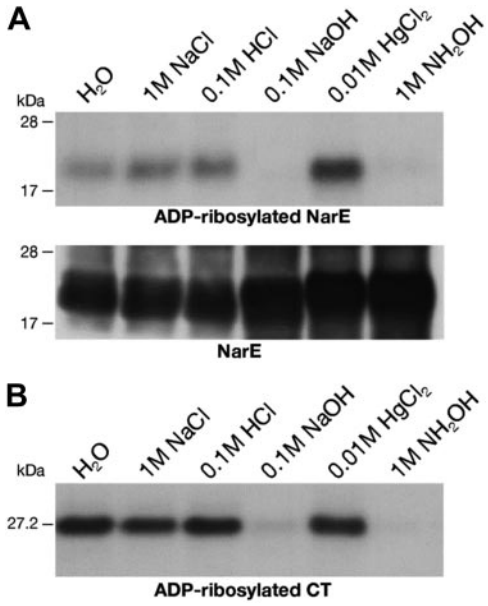

Figure 4. Chemical stability analysis indicated an arginine-ADP-ribose-linkage in auto-ADP-ribosylated NarE. *A*) After incubation at 30°C for 1 h with 100 μM [adenylate-^{32}P]NAD (2 μCi/assay), NarE (6 μg, 0.35 nmol) was precipitated with 50% TCA and left on ice for 1 h. After precipitation, the samples were centrifuged 30 min at maximum speed in a refrigerated microcentrifuge. NaCl (1 M final), HCl (0.1 M final), NaOH (0.1 M final), $HgCl_2$ (0.01 M final), and NH_2OH (1 M final) were added to pellets, and samples were incubated for another 4 h at 37°C. A control sample incubated with H_2O was also treated in the same conditions. Radiolabeled proteins were again precipitated with TCA and subjected to 4–12% SDS-PAGE in MES buffer before drying the gel for autoradiography (top panel) or Western blot (bottom panel). B) Control experiment with auto-ADP-ribosylated-CT. Positions of molecular markers are on the left. Data are representative of 3 separate experiments.

on the guanidino group of arginine (18), was also reduced by NH_2OH and NaOH (Fig. 4*B*). Radioactivity was not released from NarE by the addition of NaCl, HCl, or $HgCl_2$, suggesting that the ADP-ribosyl linkage to NarE does not involve lysine, glutamine, or cysteine (12, 19, 20).

Identification of the auto-ADP-ribosylation site

Since auto-ADP-ribosylation probably occurs at a R residue, as indicated by NH_2OH and NaOH sensitivity (Fig. 4), each R of NarE was replaced by K. All the mutants were expressed in a soluble form and recognized by polyclonal α-NarE antibodies (**Fig. 5*B***). By using the available 3D structure of NarE (8), we examined which R residues are exposed on the surface of the molecule and likely recognized as ADP-ribose acceptors by NarE. This analysis indicated that R^{124} (Fig. 5*A*) is not accessible to the solvent. Indeed, R124K replacement did not reduce ADP-ribose incorporation, showing that this residue was not modified (Fig. 5*C*). R^{97} is partially exposed and R^{33} fully exposed on the surface of NarE (Fig. 5*A*). However, the substitution of these residues did not affect ADP-ribosylation of the protein.

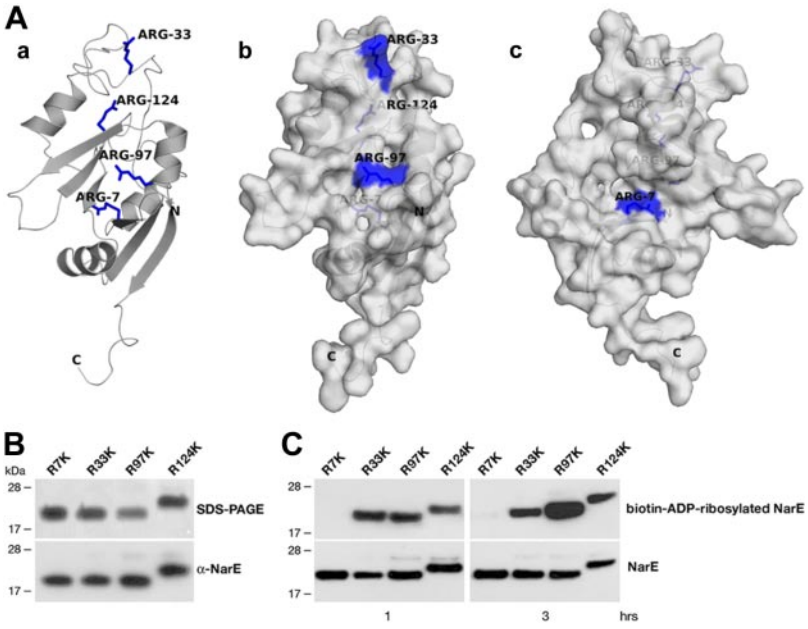

Figure 5. Site-directed mutagenesis suggested R7 as the preferred auto-ADP-ribosylation site. *A*) Solvent accessibility of the arginine residues of NarE. *a*) NarE [NarE structure protein data bank (PDB) code 2KXI] is depicted as a gray cartoon, with all R residues shown as blue sticks and labeled. N and C terminal of NarE are also labeled. *b*) Solvent-accessible surface of NarE is shown overlaid on the cartoon, using the same orientation as in *a*, and arginines are shown in blue. *c*) Same as in *b*, with rotation around the vertical axis of −90°, to show the location of R7. *B*) The 4 single RK mutants in which R7, R33, R97 or R124 replaced by K were overexpressed in *E. coli* BL21 (DE3). Purification was carried out after induction of NarE expression with IPTG by metal affinity chromatography and elution using 250 mM imidazole, as specified in Materials and Methods. Equal amounts (1 μg) of the Ni-NTA purified mutants were visualized by SDS-PAGE and Coomassie blue staining. The greater molecular mass of the R124 mutant is likely due to a partial denaturation. Immunoblot of 1 μg of purified protein using α-NarE polyclonal antibodies (1:10,000 dilution) is also shown (Western blot). Data presented are from 2 representative experiments. Positions of molecular mass standards (kDa) are indicated on the left. *C*) R7 is the auto-ADP-ribosylation site of NarE. R mutants (0.5 μg) were incubated at 30°C for 1 and 3 h (top panels) in 50 mM potassium phosphate buffer (pH 7.5) with 10 μM biotin-NAD. Control blots incubated with α-NarE polyclonal serum (1:10,000 dilution) are also shown (bottom panels).

On the other hand, replacement of R^7, which is partially exposed, with K (R7K), completely abolished auto-ADP-ribosylation after 1 or 3 h of incubation (Fig. 5*C*), suggesting that R^7 is probably the auto-ADP-ribosylation site.

Auto-ADP-ribosylation regulates ADP-ribosyltransferase and NADase activities

To define the effects of the auto-ADP-ribosylation on NarE catalytic activities, NarE was incubated with three different concentrations of NAD. After extensive dialysis to eliminate the unreacted NAD, we measured the transferase and NADase activities. Preincubation with NAD exerted a strong and dose-dependent enhancing effect on the NADase activity of NarE while decreasing the transferase activity (**Fig. 6**). Incubation of NarE with NAM or ADP-ribose, which are the products of the ADP-ribosylation reaction, prior to the assay did not change the relative transferase or NADase activities (data not shown). Incubation with NAD did not grossly alter the total amount of the two activities (Fig. 6), ruling out the inactivation or precipitation of the protein. The ratio between transferase (T) and NADase (N) activities was close to the unit when NarE was not preincubated with NAD, as described previously (6). When the protein was modified with increasing concentrations of NAD, the ratio between transferase and NADase shifted from 1 to 0.13. This shift in enzymatic activities was more evident at higher concentrations of NAD and directly correlated with the extent of automodification of NarE indicating that auto-ADP-ribosylation modulates NarE enzymatic activities.

DISCUSSION

In this report, we show that NarE represents a substrate for its ADP-ribosyltransferase activity. Auto-ADP-ribosylation of NarE modulated its catalytic activities, since addition of a negatively charged ADP-ribose to NarE led to a drastic reduction of the transferase activity, while enhancing the NADase activity. Our data provide evidence that auto-ADP-ribosylation is a specific and selective reaction and also occurs in the absence of the iron-sulfur center in the NarE structure. So far it is unknown whether eukaryotic proteins are the substrate for NarE transferase activity. However the selective expression of *narE* restricted to hypervirulent strains suggested a role in *Neisseria* pathogenesis (5). Therefore, the characterization of automodification as regulatory mechanism could be a key point to study a putative toxin. As suggested by the apparent molecular mass on Western blot and confirmed by MALDI-TOF MS analysis, which revealed a mass increase of 541 Da in agreement with the addition of a single ADP-ribose moiety, NarE appeared to be modified at a single residue. Labeling of proteins could result from the covalent association of free ADP-ribose with the ε-amino groups of K residues, which are potential ADP-ribose acceptors (12, 21, 22). We were therefore concerned that the modification could not be enzymatic, since NarE has multiple K residues and also exhibits NADase activity (6), which produces free ADP-ribose. However, ADP-ribosylation of NarE was not blocked by the addition of free ADP-ribose or the NADase inhibitor NAM (13), ruling out the possibility that ADP-ribose derived from the hydrolysis of NAD was responsible for NarE modification. While in some cases automodification can change substrate affinity (23) or amino acid target (24), NarE, in agreement with its

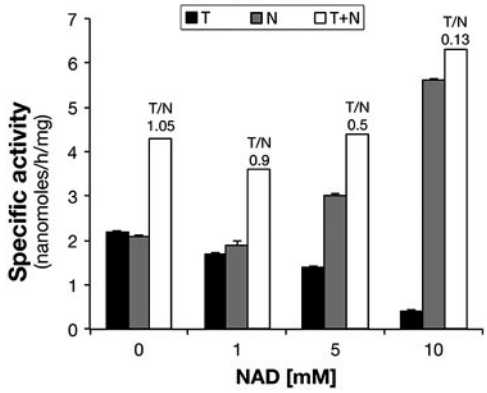

Figure 6. Auto-ADP-ribosylation decreases ADP-ribosyltransferase while enhancing NADase activity. NarE (10 μg) was incubated with 1, 5, and 10 mM NAD for 18 h at 30°C, followed by extensive dialysis with 50 mM potassium phosphate buffer (pH 7.5). ADP-ribosyltransferase activity of NarE was assayed using a filter plate-based assay performed in a total volume of 0.3 ml in 50 mM potassium phosphate buffer (pH 7.5), with 0.6 mg of polyarginine and 0.1 mM [adenine-^{14}C]NAD (0.05 μCi). The incorporated radioactivity was measured in a Packard TopCount counter. Values are means ± SD from 3 independent experiments performed in quadruplicate. NADase activity assay was carried out in 50 mM potassium phosphate buffer (pH 7.5) and 0.1 mM [carbonyl-^{14}C]NAD (0.05 μCi) in a total volume of 0.3 ml. Samples (100 μl) after incubation at 30°C were applied to 1-ml column of Dowex AG 1-X2, and ^{14}C-nicotinamide was eluted with 5 ml of H_2O for liquid scintillation counting. ADP-ribosyltransferase (T, black bars), NADase (N, dark gray bars), and sum of the two calculated activities (T+N, light gray bars) are reported as nanomoles per hour per milligram of NarE. Ratio between ADP-ribosyltransferase and NADase activities is indicated as T/N. Data are means ± SD of values from 3 independent experiments performed in duplicate.

specificity, used R as ADP-ribose acceptor, as indicated by the strong instability of the ADP-ribosyl-linkage in the presence of NH_2OH and NaOH (15). Analysis of NarE mutants indicated that R^7 could be the auto-ADP-ribosylation site, although we failed to obtain more direct evidence through mass spectrometry. This arginine residue is located in region I of the ART group and has a critical role in NAD binding and catalysis in ART family members (25–28) and in NarE (8). Auto-ADP-ribosylation activity has also been shown as a mechanism of regulation for other ARTs, including the rat ecto-ADP-ribosyltransferase 2.2 (29–31), the human ART5 (24) and the *P. aeruginosa* exoenzyme S (32). Interestingly, the addition of ADP-ribose to NarE markedly affects its enzymatic activities. The reduction in transferase activity is proportionally correlated with the increase in NADase activity. In addition, the ratio between transferase and NADase activities shifts from 1 to 0.13 when the protein is modified with increasing concentrations of NAD, suggesting a direct link between the increase in NADase activity and auto-ADP-ribosylation. Glycohydrolase activity, consisting of the hydrolysis of NAD in the absence of a target substrate, is found in many bacterial and mammalian ARTs, but its physiological relevance is still unknown. Lieberman (33) first hypothesized that auto-ADP-ribosylation could be involved in the mechanism of regulation of the NADase activity. More recently, similar observations were made for the bovine (34) and rabbit erythrocyte enzyme (35), the human ART5 (24), and the NADase expressed on the surface of lung epithelial cells (36). The attachment of a single moiety of ADP-ribose, which carries two negative charges, causes a remarkable change in the chemical properties of R, since at neutral pH the R is positively charged. When we mutagenized the R^7 residue, to K, the NarE mutant lost completely both activities, likely due to a reduced NAD binding (8). The decrease of transferase activity supports the hypothesis that the link of ADP-ribose to R^7 is important for the enzyme-ADP-ribose acceptor substrate interaction. Glycohydrolase activity of NarE shows that the active site is not altered and the binding with NAD does occur. The increase in NADase activity resulting from auto-ADP-ribosylation may reduce concentration of NAD available for NAD transfer on exogenous protein substrates and for cellular functions. Recent observations indicated that NarE protein was expressed in the outer membrane vesicles (OMVs) of hypervirulent clones. The neutrophil mediated killing of OMVs was impaired by the presence of NarE (37). These data strongly suggested a role of NarE during *Neisseria* invasion. The cytotoxycity of ADP-ribosylating toxins is usually associated with transferase activity. Our unpublished data indicated that NarE transferase activity is enhanced *in vitro* by the presence of Fe^{3+}. Thus, NarE could use the transferase activity as a pathogenetic mechanism in the presence of Fe^{3+} with the formation of a stable cluster. However, auto-ADP-ribosylation can enhance the pathogenicity of *Neisseria* in the absence of iron, enhancing its NADase activity. In this case, the pathogenesis of *Neisseria* could be associated with the NADase reaction, as it occurs in group A streptococci (GAS; ref. 38). The data reported in this study provide evidence of a unique regulation of enzymatic activities and indicate that this mechanism may have a role in the invasive infection of many hypervirulent clonal complexes. FJ

The authors thank Giorgio Corsi for his unstinting help with artwork; Elisabetta Soldaini for helpful discussion, valuable advice, and assistance; and Enrico Malito for the analysis of the 3D structure. The work was financially supported by Novartis Vaccines and Diagnostics.

REFERENCES

1. Johnson, A. P. (1983) The pathogenic potential of commensal species of *Neisseria*. *J. Clin. Pathol.* **36,** 213–223
2. Masignani, V., Balducci, E., Serruto, D., Veggi, D., Arico, B., Comanducci, M., Pizza, M., and Rappuoli, R. (2004) In silico identification of novel bacterial ADP-ribosyltransferases. *Int. J. Med. Microbiol.* **293,** 471–478
3. Ueda, K., and Hayaishi, O. (1985) ADP-ribosylation. *Annu. Rev. Biochem.* **54,** 73–100
4. Moss, J., and Vaughan, M. (1988) ADP-ribosylation of guanyl nucleotide-binding regulatory proteins by bacterial toxins. *Adv. Enzymol. Relat. Areas Mol. Biol.* **61,** 303–379
5. Tettelin, H., Saunders, N. J., Heidelberg, J., Jeffries, A. C., Nelson, K. E., Eisen, J. A., Ketchum, K. A., Hood, D. W., Peden, J. F., Dodson, R. J., Nelson, W. C., Gwinn, M. L., DeBoy, R., Peterson, J. D., Hickey, E. K., Haft, D. H., Salzberg, S. L., White,

O., Fleischmann, R. D., Dougherty, B. A., Mason, T., Ciecko, A., Parksey, D. S., Blair, E., Cittone, H., Clark, E. B., Cotton, M. D., Utterback, T. R., Khouri, H., Qin, H., Vamathevan, J., Gill, J., Scarlato, V., Masignani, V., Pizza, M., Grandi, G., Sun, L., Smith, H. O., Fraser, C. M., Moxon, E. R., Rappuoli, R., and Venter, J. C. (2000) Complete genome sequence of *Neisseria meningitidis* serogroup B strain MC58. *Science* **287,** 1809–1815

6. Masignani, V., Balducci, E., Di Marcello, F., Savino, S., Serruto, D., Veggi, D., Bambini, S., Scarselli, M., Arico, B., Comanducci, M., Adu-Bobie, J., Giuliani, M. M., Rappuoli, R., and Pizza, M. (2003) NarE: a novel ADP-ribosyltransferase from *Neisseria meningitidis*. *Mol. Microbiol.* **50,** 1055–1067
7. Del Vecchio, M., Pogni, R., Baratto, M. C., Nobbs, A., Rappuoli, R., Pizza, M., and Balducci, E. (2009) Identification of an iron-sulfur cluster that modulates the enzymatic activity in NarE, a *Neisseria meningitidis* ADP-ribosyltransferase. *J. Biol. Chem.* **284,** 33040–33047
8. Koehler, C., Carlier, L., Veggi, D., Balducci, E., Di Marcello, F., Ferrer-Navarro, M., Pizza, M., Daura, X., Soriani, M., Boelens, R., and Bonvin, A. M. (2011) Structural and biochemical characterization of NarE, an iron-containing ADP-ribosyltransferase from *Neisseria meningitidis*. *J. Biol. Chem.* **286,** 14842–14851
9. Balducci, E. (2005) A filter plate-based assay for mono adenosine 5′-diphosphate-ribosyltransferases. *Anal. Biochem.* **344,** 278–280
10. Moss, J., Manganiello, V. C., and Vaughan, M. (1976) Hydrolysis of nicotinamide adenine dinucleotide by choleragen and its A protomer: possible role in the activation of adenylate cyclase. *Proc. Natl. Acad. Sci. U. S. A.* **73,** 4424–4427
11. Banasik, M., Komura, H., Shimoyama, M., and Ueda, K. (1992) Specific inhibitors of poly(ADP-ribose) synthetase and mono-(ADP-ribosyl)transferase. *J. Biol. Chem.* **267,** 1569–1575
12. Cervantes-Laurean, D., Minter, D. E., Jacobson, E. L., and Jacobson, M. K. (1993) Protein glycation by ADP-ribose: studies of model conjugates. *Biochemistry* **32,** 1528–1534
13. Zatman, L. J., Kaplan, N. O., Colowick, S. P., and Ciotti, M. M. (1954) The isolation and properties of the isonicotinic acid hydrazide analogue of diphosphopyridine nucleotide. *J. Biol. Chem.* **209,** 467–484
14. Vogelsgesang, M., and Aktories, K. (2006) Exchange of glutamine-217 to glutamate of Clostridium limosum exoenzyme C3 turns the asparagine-specific ADP-ribosyltransferase into an arginine-modifying enzyme. *Biochemistry* **45,** 1017–1025
15. Kreimeyer, A., Adamietz, P., and Hilz, H. (1985) Alkylation-induced mono(ADP-ribosyl)-histones H1 and H2B. Hydroxylamine-resistant linkage in hepatoma cells. *Biol. Chem. Hoppe Seyler* **366,** 537–544
16. Hsia, J. A., Tsai, S. C., Adamik, R., Yost, D. A., Hewlett, E. L., and Moss, J. (1985) Amino acid-specific ADP-ribosylation. Sensitivity to hydroxylamine of [cysteine(ADP-ribose)]protein and [arginine(ADP-ribose)]protein linkages. *J. Biol. Chem.* **260,** 16187–16191
17. Moss, J., Yost, D. A., and Stanley, S. J. (1983) Amino acid-specific ADP-ribosylation. *J. Biol. Chem.* **258,** 6466–6470
18. Gill, D. M., and Woolkalis, M. J. (1991) Cholera toxin-catalyzed [32P]ADP-ribosylation of proteins. *Methods Enzymol.* **195,** 267–280
19. Meyer, T., Koch, R., Fanick, W., and Hilz, H. (1988) ADP-ribosyl proteins formed by pertussis toxin are specifically cleaved by mercury ions. *Biol. Chem. Hoppe Seyler* **369,** 579–583
20. Cervantes-Laurean, D., Loflin, P. T., Minter, D. E., Jacobson, E. L., and Jacobson, M. K. (1995) Protein modification by ADP-ribose via acid-labile linkages. *J. Biol. Chem.* **270,** 7929–7936
21. Jacobson, E. L., Cervantes-Laurean, D., and Jacobson, M. K. (1994) Glycation of proteins by ADP-ribose. *Mol. Cell. Biochem.* **138,** 207–212
22. Jacobson, E. L., Cervantes-Laurean, D., and Jacobson, M. K. (1997) ADP-ribose in glycation and glycoxidation reactions. *Adv. Exp. Med. Biol.* **419,** 371–379
23. Yamada, K., Tsuchiya, M., Nishikori, Y., and Shimoyama, M. (1994) Automodification of arginine-specific ADP-ribosyltransferase purified from chicken peripheral heterophils and alteration of the transferase activity. *Arch. Biochem. Biophys.* **308,** 31–36
24. Weng, B., Thompson, W. C., Kim, H. J., Levine, R. L., and Moss, J. (1999) Modification of the ADP-ribosyltransferase and NAD glycohydrolase activities of a mammalian transferase (ADP-ribosyltransferase 5) by auto-ADP-ribosylation. *J. Biol. Chem.* **274,** 31797–31803
25. Domenighini, M., Magagnoli, C., Pizza, M., and Rappuoli, R. (1994) Common features of the NAD-binding and catalytic site of ADP-ribosylating toxins. *Mol. Microbiol.* **14,** 41–50
26. Domenighini, M., and Rappuoli, R. (1996) Three conserved consensus sequences identify the NAD-binding site of ADP-ribosylating enzymes, expressed by eukaryotes, bacteria and T-even bacteriophages. *Mol. Microbiol.* **21,** 667–674
27. Fieldhouse, R. J., and Merrill, A. R. (2008) Needle in the haystack: structure-based toxin discovery. *Trends. Biochem. Sci.* **33,** 546–556
28. Van, D. A. F., Merritt, E. A., Pizza, M., Domenighini, M., Rappuoli, R., and Hol, W. G. (1995) The Arg7Lys mutant of heat-labile enterotoxin exhibits great flexibility of active site loop 47–56 of the A subunit. *Biochemistry* **34,** 10996–11004
29. Koch-Nolte, F., Petersen, D., Balasubramanian, S., Haag, F., Kahlke, D., Willer, T., Kastelein, R., Bazan, F., and Thiele, H. G. (1996) Mouse T cell membrane proteins Rt6-1 and Rt6-2 are arginine/protein mono(ADPribosyl)transferases and share secondary structure motifs with ADP-ribosylating bacterial toxins. *J. Biol. Chem.* **271,** 7686–7693
30. Rigby, M. R., Bortell, R., Stevens, L. A., Moss, J., Kanaitsuka, T., Shigeta, H., Mordes, J. P., Greiner, D. L., and Rossini, A. A. (1996) Rat RT6.2 and mouse Rt6 locus 1 are NAD+: arginine ADP ribosyltransferases with auto-ADP ribosylation activity. *J. Immunol.* **156,** 4259–4265
31. Hara, N., Tsuchiya, M., and Shimoyama, M. (1996) Glutamic acid 207 in rodent T-cell RT6 antigens is essential for arginine-specific ADP-ribosylation. *J. Biol. Chem.* **271,** 29552–29555
32. Riese, M. J., Goehring, U. M., Ehrmantraut, M. E., Moss, J., Barbieri, J. T., Aktories, K., and Schmidt, G. (2002) Auto-ADP-ribosylation of Pseudomonas aeruginosa ExoS. *J. Biol. Chem.* **277,** 12082–12088
33. Lieberman, I. (1957) The mechanism of the specific depression of an enzyme activity in cells in tissue culture. *J. Biol. Chem.* **225,** 883–898
34. Pekala, P. H., Yost, D. A., and Anderson, B. M. (1980) Self-inactivation of an erythrocyte NAD glycohydrolase. *Mol. Cell. Biochem.* **31,** 49–56
35. Han, M. K., Lee, J. Y., Cho, Y. S., Song, Y. M., An, N. H., Kim, H. R., and Kim, U. H. (1996) Regulation of NAD+ glycohydrolase activity by NAD(+)-dependent auto-ADP-ribosylation. *Biochem. J.* **318,** 903–908
36. Balducci, E., and Micossi, L. G. (2002) NAD-dependent inhibition of the NAD-glycohydrolase activity in A549 cells. *Mol. Cell. Biochem.* **233,** 127–132
37. Günther F., Lappan M., Lein N., Claus H., and Vogel, U. (2012) Impact of *Neisseria meningitidis* outer membrane vesicles (OMV) on immune response by polymorphonuclear neutrophils (PMN). Poster presentation P204, XVIIIth International Pathogenic Neisseria Conference (IPNC), Wurzburg, Germany.
38. Bricker, A. L., Carey, V. J., and Wessels, M. R. (2005) Role of NADase in virulence in experimental invasive group A streptococcal infection. *Infect. Immun.* **73,** 6562–6566

Received for publication March 18, 2013.
Accepted for publication August 5, 2013.